



UvA-DARE (Digital Academic Repository)

The Arabidopsis leucine-rich repeat receptor-like kinase MIK2 is a crucial component of early immune responses to a fungal-derived elicitor

Coleman, A.D.; Maroschek, J.; Raasch, L.; Takken, F.L.W.; Ranf, S.; Hückelhoven, R.

DOI

[10.1111/nph.17122](https://doi.org/10.1111/nph.17122)

Publication date

2021

Document Version

Final published version

Published in

New Phytologist

License

CC BY-NC

[Link to publication](#)

Citation for published version (APA):

Coleman, A. D., Maroschek, J., Raasch, L., Takken, F. L. W., Ranf, S., & Hückelhoven, R. (2021). The Arabidopsis leucine-rich repeat receptor-like kinase MIK2 is a crucial component of early immune responses to a fungal-derived elicitor. *New Phytologist*, 229(6), 3453-3466. <https://doi.org/10.1111/nph.17122>

General rights

It is not permitted to download or to forward/distribute the text or part of it without the consent of the author(s) and/or copyright holder(s), other than for strictly personal, individual use, unless the work is under an open content license (like Creative Commons).

Disclaimer/Complaints regulations

If you believe that digital publication of certain material infringes any of your rights or (privacy) interests, please let the Library know, stating your reasons. In case of a legitimate complaint, the Library will make the material inaccessible and/or remove it from the website. Please Ask the Library: <https://uba.uva.nl/en/contact>, or a letter to: Library of the University of Amsterdam, Secretariat, Singel 425, 1012 WP Amsterdam, The Netherlands. You will be contacted as soon as possible.

UvA-DARE is a service provided by the library of the University of Amsterdam (<https://dare.uva.nl>)

The *Arabidopsis* leucine-rich repeat receptor-like kinase MIK2 is a crucial component of early immune responses to a fungal-derived elicitor

Alexander D. Coleman¹ , Julian Maroschek¹ , Lars Raasch¹, Frank L.W. Takken² , Stefanie Ranf¹  and Ralph Hückelhoven¹ 

¹Phytopathology, TUM School of Life Sciences Weihenstephan, Technical University of Munich, Freising 85354, Germany; ²Molecular Plant Pathology, SILS, University of Amsterdam, PO Box 94215, Amsterdam 1090 GE, the Netherlands

Author for correspondence:
Ralph Hückelhoven
Email: hueckelhoven@wzw.tum.de

Received: 5 October 2020
Accepted: 23 November 2020

New Phytologist (2021) 229: 3453–3466
doi: 10.1111/nph.17122

Key words: *Arabidopsis thaliana*, fungal elicitor, *Fusarium*, leucine-rich repeat receptor-like kinase, MDIS1-INTERACTING RECEPTOR LIKE KINASE 2, pattern-recognition receptor, pattern-triggered immunity, plant immunity.

Summary

- *Fusarium* spp. cause severe economic damage in many crops, exemplified by Panama disease of banana or *Fusarium* head blight of wheat. Plants sense immunogenic patterns (termed elicitors) at the cell surface to initiate pattern-triggered immunity (PTI). Knowledge of fungal elicitors and corresponding plant immune-signaling is incomplete but could yield valuable sources of resistance.
- We characterized *Arabidopsis thaliana* PTI responses to a peptide elicitor fraction present in several *Fusarium* spp. and employed a forward-genetic screen using plants containing a cytosolic calcium reporter to isolate *fusarium elicitor reduced elicitation* (*fer*) mutants.
- We mapped the causal mutation in *fer1* to the leucine-rich repeat receptor-like kinase MDIS1-INTERACTING RECEPTOR-LIKE KINASE 2 (MIK2) and confirmed a crucial role of MIK2 in fungal elicitor perception. MIK2-dependent elicitor responses depend on known signaling components and transfer of *AtMIK2* is sufficient to confer elicitor sensitivity to *Nicotiana benthamiana*.
- *Arabidopsis* senses *Fusarium* elicitors by a novel receptor complex at the cell surface that feeds into common PTI pathways. These data increase mechanistic understanding of PTI to *Fusarium* and place MIK2 at a central position in *Arabidopsis* elicitor responses.

Introduction

Fusarium fungi form a large species complex that includes a number of economically important plant pathogens. Current global outbreaks of Panama disease caused by *Fusarium oxysporum* f. sp. *cubense* Tropical Race 4 (*Foc* TR4) critically threaten banana production worldwide and provide a prime example of the devastating properties of the *Fusarium* wilt pathogen (Dita *et al.*, 2018). Major resistance (*R*) genes have been used widely in agriculture to provide effective and highly specific pathogen resistance, but as the corresponding recognized effectors (avirulence-genes) from the pathogen can be readily lost or altered by mutation, these genes rapidly become ineffective (McDonald & Linde, 2002). For example, various resistance genes of tomato have been overcome by different *Fusarium* wilt races (de Sain & Rep, 2015). In many crops, genetic sources of resistance against *Fusarium* spp. are scarce, or they provide quantitative resistance such as *Fhb1* in wheat against *Fusarium* head blight (Hao *et al.*, 2020). Transgenic resistance to Panama disease has been demonstrated successfully, yet no genetic resistance is currently available in commercial banana and no fungicide or biocontrol measure has proven effective (Dale *et al.*, 2017). Targeted fundamental

research into plant nonrace-specific basal immunity against *Fusarium* fungi represents one strategy to develop novel sources of quantitative resistance which may be applicable to a broad spectrum of pathosystems and more durable than those mediated by a specific resistance locus.

Plants have evolved diverse pattern-recognition receptors (PRRs) at the cell surface to detect microbial invaders and form multipartite PRR complexes to initiate and regulate intracellular signaling pathways (Couto & Zipfel, 2016). Molecular patterns from diverse origins (modified-self or nonself; collectively termed elicitors) can be perceived by plant PRRs contributing to quantitative disease-resistance via the activation of pattern-triggered immunity (PTI) (Boller & Felix, 2009). Various elicitors from bacteria, fungi and oomycetes are perceived by plants and initiate PTI responses (Saijo *et al.*, 2018). Plants differ substantially in their capacity to recognize and respond to different elicitors, suggesting a rich diversity of PRRs and their cognate microbial ligands, many of which remain unidentified. Much of our current understanding of PTI in plants comes from *Arabidopsis thaliana* where several PRRs and associated signaling components have been identified. A classic example is the PRR FLAGELLIN-SENSITIVE 2 (FLS2), which recognizes bacterial flagellin or its

conserved peptide derivatives (e.g. flg22) (Felix *et al.*, 1999; Gomez-Gomez & Boller, 2000). A wealth of genetic resources and well-established PTI marker assays make *Arabidopsis* a highly amenable system towards identifying novel immunity components and determining their role in known signaling pathways.

The most prominent fungal-derived elicitor is the cell wall component chitin and other examples include endopolygalacturonases (PGs), ethylene-inducing xylanase (EIX), and *Sclerotinia* culture filtrate elicitor 1 (SCFE1) (Ron & Avni, 2004; Zhang *et al.*, 2013; Zhang *et al.*, 2014; Sanchez-Vallet *et al.*, 2015). A conserved 20 amino acid (AA) pattern from NEP1-like proteins (NLPs) – referred to as nlp20 – present in many fungal, oomycete and bacterial species also triggers immune responses in various dicotyledonous plant species (Boehm *et al.*, 2014; Oome *et al.*, 2014). Nonrace-specific elicitors derived from *Fusarium* spp. cell walls or culture filtrates have been shown to elicit typical PTI responses in diverse plant systems (Ndimba *et al.*, 2003; Chivasa *et al.*, 2005; Davies *et al.*, 2006; Dey *et al.*, 2009; Kesten *et al.*, 2019; Li *et al.*, 2019a,b). Nevertheless, specific knowledge of elicitors from *Fusarium* spp. and corresponding plant immunity components is sparse.

In order to identify novel components involved in nonrace-specific immunity to *Fusarium* spp., we generated an elicitor-active extract from diverse *Fusarium* spp. that induces PTI marker responses in *Arabidopsis* and used this to screen for mutants with compromised immune responses. This revealed a mutant strongly impaired in PTI responses to *Fusarium* extracts yet fully responsive to other fungal elicitors. We identified a causal mutation in the leucine-rich repeat receptor-like kinase MIK2, which was described previously in the context of abiotic and biotic stress resistance, sexual reproduction and cell-wall integrity sensing (Julkowska *et al.*, 2016; Wang *et al.*, 2016; Van der Does *et al.*, 2017; Engelsdorf *et al.*, 2018). Importantly, MIK2 also contributes to *Arabidopsis* resistance against *F. oxysporum* (Van der Does *et al.*, 2017). Here, we describe a new function of MIK2 in early immune responses to extracts from *Fusarium* spp.

Materials and Methods

Plant material and growth conditions

All plant material used for this study is listed in Supporting Information Table S1. For growth in liquid medium, *Arabidopsis thaliana* seeds were surface-sterilized, stratified for at least 48 h (dark; 4°C) and grown under long-day conditions (16 h : 8 h, light : dark photoperiod; 20–22°C) in liquid MS medium (½ Murashige & Skoog medium plus vitamins (Duchefa, Haarlem, Holland), 0.25% sucrose, 1 mM MES, pH 5.7). The *A. thaliana* plants for reactive oxygen species (ROS) measurements were sown on a soil/vermiculite mix (8 : 1), stratified for 2 d (dark; 4°C) and grown under short-day conditions (8 h : 16 h, light : dark photoperiod; 20–22°C; 55% RH). *Nicotiana benthamiana* plants for transient expression assays were grown on soil under long-day conditions (16 h : 8 h, light : dark photoperiod; 21–23°C; 55% RH).

Fusarium elicitor preparation, enrichment and characterization

Fusarium graminearum (isolate Fg006) is part of the TUM Phytopathology collection and *Fusarium oxysporum* (isolate DSM 62292) was kindly provided by Ludwig Niessen (TU Munich, Germany). *Trichoderma atroviride* (isolate SZMC 20780) was kindly provided by Laszlo Kredics (University of Szeged, Hungary). Fungal strains were grown in liquid malt medium (3% malt extract, 0.3% peptone) or synthetic liquid medium (Gotthardt *et al.*, 2020) at 25°C on a 70 rpm shaker for 7–10 d. Fungal mycelium was washed thoroughly with distilled water, then lyophilized and ground.

For preparation of FGE (*Fusarium graminearum* elicitor), FOE (*Fusarium oxysporum* elicitor) or TAE (*Trichoderma atroviride* elicitor), mycelial powder was dissolved in water and autoclaved for 20 min at 121°C. The soluble fraction was concentrated and desalted using PD-10 desalting columns (GE Healthcare, Chicago, IL, USA). Crude elicitor fractions (i.e. FGE/FOE) were quantified based on the weight of starting material used (mg lyophilized mycelium ml⁻¹).

For the preparation of enriched elicitor fractions (EnFOE and EnTAE), the soluble fraction obtained above was dialyzed in Ø22-mm tubing with a 14 kDa cut-off (Biomol, Hamburg, Germany) overnight at 4°C then lyophilized. The powder was dissolved in water, desalted, then incubated 1 : 2 with Macro-Prep High Q anion exchange media (Bio-Rad) on a shaker at RT for 1 h. ‘Q_{unbound}’ fractions (supernatant and subsequent water washes) were concentrated, desalted and incubated 1 : 2 with Macro-Prep High S cation exchange media (Bio-Rad). Samples were eluted using 0.5 M NaCl and lyophilized. Finally, the ‘Q_{unbound/Seluate}’ powder was dissolved in water and desalted. Protein concentration was determined using a Pierce™ BCA Protein Assay Kit (Thermo Scientific, Waltham, MA, USA).

For *F. oxysporum* culture filtrate (FOCF) preparation, *F. oxysporum* was grown in synthetic liquid medium for 10 d and mycelium/spores removed using filter paper followed by centrifugation. One liter of supernatant was autoclaved, lyophilized, resuspended to 15 ml with water, then twice desalted to 60 ml. Preparations were filtered through a membrane with a 5 kDa cut-off (Vivaspin 2; Sartorius Stedim Lab Ltd, Stonehouse, UK) and the > 5 kDa fraction was used for experiments.

For proteinase treatment, elicitor samples were incubated overnight at 50°C ± proteinase K (10 µg ml⁻¹; Carl Roth GmbH, Karlsruhe, Germany) then heat-inactivated for 15 min at 95°C. To determine protein kinase dependency, Col-0^{AEC} seedlings were pre-treated with K252a (10 µM; Sigma-Aldrich) or DMSO as a solvent-only control 30 min before elicitor application.

Elicitors

Chitin derived from shrimp shell (C9752; Sigma-Aldrich) was ground and re-suspended in water for experiments. Flg22 (QRLSTGSRINSAKDDAAGLQIA), Pep1 (ATKVKAKQRGKEKVSSGRPGQHN) and the Nep-1-like peptide from

F. oxysporum (FoNLP; AIMYAWYWPkdQPADGNLVSgHR) were synthesized on an Abimed EPS221 system (Abimed, Langenfeld, Germany). RALF17 (NSIGAPAMREDLPKGCA PGSSAGCKMQPANPYKPGCEASQRCRGG) was ordered from Pepmic Corp. Ltd (Suzhou, China).

Detection of ROS in *A. thaliana* leaf discs

Leaf discs (Ø4-mm) from 6–8-wk-old soil-grown plants were floated overnight on 200 µl water in 96-well plates (dark; RT). Before the measurement, water was replaced with 75 µl of a 2 µg ml⁻¹ horseradish peroxidase (type II; Roche) and 5 µM L-012 (WAKO Chemicals, Neuss, Germany) solution. Luminescence was recorded as relative light units (rlu) at 1 min intervals with a Luminoskan Ascent 2.1 (Thermo Scientific) or a Tecan F200 (Tecan, Männedorf, Switzerland) luminometer. Measurements consisted of a 10 min background reading then a 60-min reading after elicitor application to the appropriate final concentration. Recorded values were normalized to average ROS measured over the last 5 min before elicitor treatment followed by subtraction of values for mock-treated controls (included for each genotype on the same plate). Individual measurements over the 60 min (kinetics) after elicitation (time point (T)0) or the highest luminescence achieved (maxima) were used for analyses. To compare elicitor responses between mutant genotypes measured on separate plates, values were normalized to the mean maximum rlu measured in respective wild-type (WT) controls from each plate (set to 1; dashed line in Fig. 2a–c and Fig. S8a–c). Statistical analysis of maximum ROS (unpaired Student's *t*-test to respective WT control with two-tailed *P*-value) was performed using PRISM 8.0.1 (Graphpad Software, San Diego, CA, USA). Measurement of RALF peptide-induced ROS was performed according to Stegmann *et al.* (2017) on a Tecan F200 luminometer.

Aequorin luminescence measurements

Eight-day-old liquid-grown apoaequorin-expressing seedlings were placed individually in 96-well plates containing 100 µl of 5 µM coelenterazine-h (PJK, Kleinblittersdorf, Germany) overnight (dark; RT). Resting luminescence intensities were determined by scanning each well 12 times at 10 s intervals, then a 25 µl elicitor preparation was added at the appropriate concentrations and luminescence measured 180 times at 10 s intervals (Luminoskan Ascent 2.1). The remaining aequorin was discharged using 150 µl discharge solution (2 M CaCl₂, 20% ethanol) per well. Cytosolic elevations of calcium ion concentration ($[Ca^{2+}]_{cyt}$) were calculated as L/L_{max} (luminescence counts per second (*L*) relative to total luminescence counts remaining (L_{max})) as described previously (Ranf *et al.*, 2012). For $[Ca^{2+}]_{cyt}$ measurements in different plant tissues, 9-d-old seedlings grown vertically on solid MS medium (as described above with 0.9% agarose; Sigma-Aldrich) were dissected and respective tissues incubated in substrate as indicated above. Individual measurements over 30 min (kinetics) after elicitation (i.e. T0) or the highest luminescence achieved (maxima) were used for analyses.

Statistical analysis of maximum $[Ca^{2+}]_{cyt}$ (L/L_{max}) (unpaired Student's *t*-test to respective WT control with two-tailed *P* value) was performed using PRISM 8.0.1.

Immunoblot analysis of mitogen-activated protein kinase phosphorylation

Fourteen-day-old liquid-grown seedlings were equilibrated for 24 h in fresh MS medium then elicitor solutions were added to the appropriate concentrations and seedlings were harvested at the stated time points. Proteins were extracted (50 mM Tris-HCl pH 7.5, 100 mM NaCl, 20 mM EDTA, 30 mM glycerophosphate, 30 mM 4-NPP, 20 mM MgCl₂, 4 mM NaF, 4 mM Na₃VO₄, 4 mM Na₂MoO₄, 10 mM DTT, 0.2% Tween-20, 1% protease inhibitor (P9599; Sigma)), quantified, then boiled in SDS sample buffer (50 mM Tris-HCl pH 6.8, 1% β-Mercaptoethanol, 2% SDS, 0.1% bromophenol blue, 10% glycerol). Proteins were separated by SDS-PAGE and transferred to a suitable membrane. Immunoblotting with an antibody against phosphorylated mitogen-activated protein kinases (MAPKs) (p44/42; 9101; Cell Signaling Technology, Leiden, the Netherlands) was performed. Blots were visualized using SuperSignal West Dura Substrate (Thermo Scientific) in a Fusion SL Imager (Vilber Lourmat, Eberhardzell, Germany) with the accompanying software. Amido Black staining confirmed equal protein loading and blotting (50 µg total protein per sample; a Rubisco band of c. 56 kDa is shown).

Gene-expression analysis

Ten-day-old liquid-grown seedlings were equilibrated in fresh MS medium for 24 h before water or elicitor treatment at the stated final concentrations. Whole seedlings were harvested at 2 h and total RNA was extracted using a conventional Trizol/chloroform method. RNA was treated with DNaseI then reverse-transcribed using oligo(dT) and RevertAid reverse transcriptase (Thermo Scientific). Complementary DNA was mixed together with SYBR Green™ (Thermo Scientific) and gene-specific primers (Table S2) then quantitative reverse-transcription (qRT)-PCR performed using an ARIAMX Real-Time PCR system (G8830A instrument; Agilent) and the accompanying software (v1.5). Target gene expression was calculated in EXCEL 2010 (Microsoft, Redwood, WA, USA) using the 2^{-ΔΔCT} method described by Livak & Schmittgen (2001) and normalized to the house-keeping gene *Ubiquitin 5* (*UBQ5*). Mean values from two technical replicates included for each sample–primer combination were used for analysis. Data represent relative expression of each target gene compared to the water-treated control for each genotype.

Arabidopsis thaliana mutant screen

Col-0^{A^{EQ}} mutant screening was performed similar to previous studies (Ranf *et al.*, 2012, 2015). Seeds were treated with 0.3% ethyl methane sulfonate (EMS; Sigma-Aldrich), grown on soil and harvested individually. 12–24 M₂ seedlings per M₁ plant

were measured for aequorin luminescence in response to FGE as described above but without discharge. FGE was used as we initiated screening before elicitor enrichment. Seedlings with impaired elevations in aequorin luminescence were 'rescued' to solid MS media and later transferred to soil for seed production. Mutant phenotypes were verified by quantitative $[Ca^{2+}]_{cyt}$ measurements on corresponding M_3 offspring. *Fusarium elicitor reduced elicitation 1 (fere1)* was backcrossed (Col-0^{AEQ}) to reduce background mutations and a single F_2 offspring homozygous for *fere1* was used for all experiments and subsequent genetic material produced in this study.

Mapping and sequencing of candidate genes

Approximately 200 *fere1* × Landsberg *erecta-0* (Ler-0) F_2 were grown on soil for seed setting. F_3 progeny were phenotyped using quantitative $[Ca^{2+}]_{cyt}$ measurements and harvested in pools (25–30 individuals per F_2 parent) for gDNA isolation. Pools representing 22 *fere1*-like F_2 and five WT-like F_2 individuals were used for mapping. The analysis of PCR-based markers localized *FERE1* to a mapping interval of approximately 0.4 Mbp (position: 5372922–5756738) on chromosome 4 containing 121 gene loci (TAIR v.10; <https://www.arabidopsis.org/>) including the *MDIS1-INTERACTING RECEPTOR-LIKE KINASE 2 (MIK2)* gene locus (position: 5636479–5640952). A W876STOP mutation in *fere1* was confirmed by sequencing and a derived cleaved amplified polymorphic sequence (dCAPS) marker was developed to genotype the mutation (Neff *et al.*, 2002). For genotyping by dCAPS, gDNA samples were amplified by PCR with appropriate primers (Table S2) then digested at 37°C for 2 h with the enzyme *HpyF3I* (DdeI) (Thermo Scientific).

Molecular cloning and generation of transgenic lines

In order to generate a MIK2 construct with a C-terminal cMyc fusion (EQKLISEEDL) under the control of its own putative promoter, the full-length genomic fragment of *MIK2* (At4g08850) including a 2-kb upstream region was first amplified from Col-0^{AEQ} gDNA using appropriate primers (Table S2). The pENTRTM/D-TOPOTM Cloning Kit was used (Thermo Scientific) to generate a Gateway compatible entry clone then the gene was transferred into pEarleyGate303 for plant expression. To generate a *MIK2.1* construct, the MIK2 promoter and cDNA sequences were subcloned into GoldenGate modules using appropriate primers (Table S2) then assembled together into a GoldenGate-modified pCB302 binary vector for plant expression. Consequently, constructs were transferred into *Agrobacterium tumefaciens* (GV3101) and *fere1* plants were transformed by floral-dip transformation. BASTA selection on soil or MS agar plates (glufosinate-ammonium; Bayer CropScience, Langenfeld, Germany) was used to establish independent homozygous T_3 lines. The presence of cMyc-tagged MIK2 in *fere1/MIK2-cMyc* seedlings was confirmed via immunoblotting as described below.

Transient expression in *Nicotiana benthamiana* and immunoblotting

MIK2 variants with C-terminal cMyc fusions (CaMV35S promoter) were generated by GoldenGate cloning using appropriate primers (Table S2). The kinase-dead MIK2 variant (MIK2^{km}-cMyc) was generated by inserting a K802A mutation into the conserved ATP-binding site of the kinase domain via site-directed mutagenesis. The truncated MIK2 variant present in *fere1* (AA 1-875) was also generated (FERE1-cMyc). The *A. tumefaciens* (GV3101) cultures carrying the appropriate constructs were grown overnight in medium containing 100 μ M acetosyringone then harvested, washed and re-suspended in infiltration medium (10 mM MgCl₂, 10 mM MES, pH 5.7) supplemented with 150 μ M acetosyringone to an absorbance of 0.5 at 600 nm. Cell suspensions were incubated for 2 h at RT, mixed 1:1 with GV3101 carrying the p19 silencing suppressor, then infiltrated via a needle-less syringe into leaves of 6–8-wk-old *N. benthamiana* plants. ROS measurements were performed using leaf discs from infiltrated sites 48 h post-infiltration. Additional leaf discs (20 per construct and repeat) were used to generate total protein extracts for visualization of recombinant MIK2-cMyc variants. Proteins were separated by SDS-PAGE (8% gel; 75 μ g total protein per sample) and transferred to a suitable membrane. Immunoblotting with an antibody against cMyc (1:500; 13-2500; Life Technologies, Carlsbad, CA, USA) was performed overnight followed by a 2 h incubation with anti-mouse antibody conjugated to horseradish peroxidase (1:5000; sc-516102; Santa Cruz, Dallas, TX, USA). Blots were visualized on Fuji Medical X-Ray Films (100NIF; 13x18; FujiFilm, Tokyo, Japan) using SuperSignal West Femto Substrate (Thermo Scientific) then stained with Coomassie Brilliant Blue (Sigma-Aldrich) to verify equal protein loading.

Co-immunoprecipitation

BRI1-ASSOCIATED RECEPTOR KINASE 1 (BAK1) with a C-terminal green fluorescent protein (GFP) fusion (CaMV35S promoter) was generated by GoldenGate cloning using appropriate primers (Table S2). GV3101 strains carrying BAK1-GFP, MIK2-cMyc or p19 were co-infiltrated 1:1:1 into *N. benthamiana* leaves as described, followed by infiltration with EnFOE or water (mock) solutions after 3 d. Total protein was extracted (25 mM Tris-HCl pH 7.5, 150 mM NaCl, 10% glycerol, 0.5% NP-40, 1 mM EDTA, 1% PVPP, 10 mM DTT, 1 mM PMSF, 1% protease inhibitor; 30 min incubation) from infiltrated tissues 20 min after elicitation then incubated with GFP-Trap Magnetic Agarose Beads (gtma-10; Chromotek, Munich, Germany) for 2 h. Samples were washed three times (buffer as previous without addition of NP-40, PVPP and DTT) then boiled in SDS sample buffer. Immunoblotting was performed as described for cMyc, or with anti-GFP (1:500; 3H9; Chromotek) then anti-rat (1:5000; A9542; Sigma-Aldrich) antibodies.

Fusarium oxysporum infection assays

Two-week-old *Arabidopsis* seedlings were transferred to finely sieved soil containing 10K *F. oxysporum* spores per cm³ (isolate *Fo5176*). Plants were grown under 11 h : 13 h, light : dark photoperiod (28°C; 80% RH) and scored after 2 wk into three categories: Unaffected (not visibly different from mock-treated plants), affected (visibly stunted/wilted with chlorotic leaves) or decayed (no green leaf material remaining).

Results

A crude elicitor fraction from *Fusarium* species elicits typical pattern-triggered immunity (PTI) responses in *Arabidopsis*

In order to determine the feasibility of identifying *Fusarium*-relevant PTI components by forward genetics, we characterized the hallmark PTI response of cytosolic elevation of calcium ion concentration ($[Ca^{2+}]_{cyt}$) in *Arabidopsis* to crude *Fusarium graminearum* elicitor (FGE) or *Fusarium oxysporum* elicitor (FOE) fractions derived from fungal mycelium. Application of FGE or FOE to apoaequorin-expressing reporter plants (Knight *et al.*, 1991; Ranf *et al.*, 2011) induced $[Ca^{2+}]_{cyt}$ elevations, implicating the presence of elicitor activity in the extracts

(Fig. 1a). As chitin oligomers derived from fungal cell walls are potent elicitors of immune responses in plants, we tested whether the induced responses were triggered by chitin. The CHITIN ELICITOR RECEPTOR KINASE 1 mutant (*cerk1*) lacks an essential component of chitin-mediated PTI in *Arabidopsis* (Miya *et al.*, 2007) yet showed a WT response to crude *Fusarium* elicitor preparations such as FOE, indicating that chitin is not a major contributor of the responses we observed (Fig. 1b).

As crude mycelial fractions likely contain multiple elicitors that might initiate variable PTI responses, we enriched an elicitor fraction from *F. oxysporum* (EnFOE) by ion exchange resins. EnFOE gave robust and consistent responses with multiple PTI marker assays in *Arabidopsis*, including $[Ca^{2+}]_{cyt}$ elevations, ROS production, MAPK-phosphorylation and defense-marker gene activation (Fig. 1c–f). EnFOE was furthermore capable of eliciting ROS production in Brassicaceae such as *Brassica rapa* and *Capsella rubella*, as well as in barley (*Hordeum vulgare*) and in soybean (*Glycine max*), but not in the Solanaceae member *N. benthamiana* (Fig. S1). EnFOE-induced ROS responses could be abolished using a kinase inhibitor and initial biochemical characterization of EnFOE revealed that its PTI-triggering activity is sensitive to proteinase K treatment and shows a typical dose-response profile (Fig. S2a–d). EnFOE enriched from *F. oxysporum* grown in synthetic liquid medium (free from plant

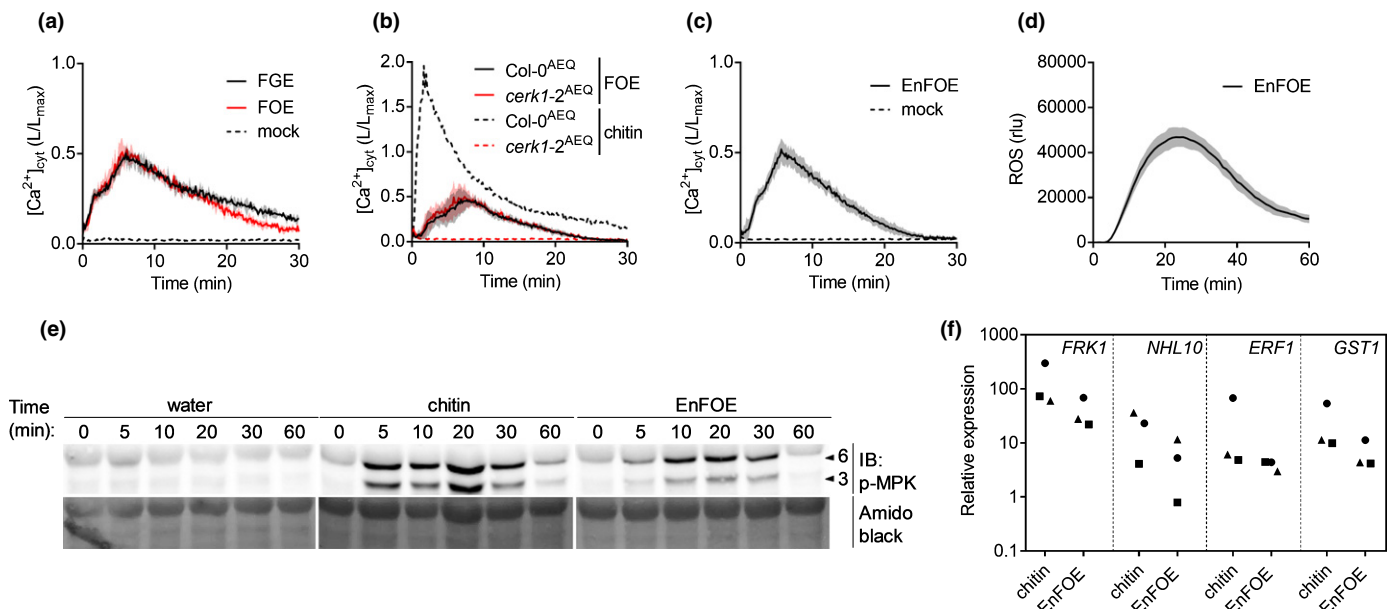


Fig. 1 *Arabidopsis thaliana* pattern-triggered immunity (PTI) marker responses to crude or enriched *Fusarium* elicitor fractions. (a) Cytosolic elevation of calcium ion concentration ($[Ca^{2+}]_{cyt}$) kinetics in Col-0^{AEQ} seedlings after elicitation with *Fusarium graminearum* elicitor (FGE) or *Fusarium oxysporum* elicitor (FOE) fractions (1 mg mycelium ml⁻¹). (b) $[Ca^{2+}]_{cyt}$ kinetics in Col-0^{AEQ} or *cerk1-2*^{AEQ} seedlings after elicitation with FGE (2.5 mg mycelium ml⁻¹; full lines) or chitin (60 µg ml⁻¹; dashed lines). (c) $[Ca^{2+}]_{cyt}$ kinetics in Col-0^{AEQ} after elicitation with enriched *F. oxysporum* elicitor (EnFOE; 0.5 µg ml⁻¹). $[Ca^{2+}]_{cyt}$ data represent mean values measured in individual seedlings over 30 min after elicitation ± SD at each measurement point (a, b: n = 3; c: n = 8). $[Ca^{2+}]_{cyt}$ kinetics indicated with a dashed line are shown without SD for clarity. (d) Reactive oxygen species (ROS) accumulation kinetics in Col-0^{AEQ} leaf discs after elicitation with EnFOE (0.5 µg ml⁻¹). Data represent mean relative light units (rlu) measured from individual leaf discs ± SD at each measurement point (n = 4). (e) Immunoblot (IB) of phosphorylated MPK6 (6) and MPK3 (3) (arrowheads at right margin; p-MPK; upper panel) in Col-0^{AEQ} seedlings after treatment with water, chitin (75 µg ml⁻¹) or EnFOE (0.5 µg ml⁻¹) over the time series stated, including Amido black staining for visualization of equal protein quantities (50 µg total protein per sample; lower panel). Data shown are from one experiment representative of three independent experiments with similar results (a–e). (f) Expression of PTI-responsive genes in Col-0^{AEQ} seedlings 2 h after treatment with chitin (75 µg ml⁻¹) or EnFOE (0.5 µg ml⁻¹) relative to expression in water-treated plants (set at 1; symbols represent three independent experiments; target genes normalized to *UBQ5*).

peptides) also gave comparable PTI responses in Arabidopsis including ROS production, confirming that the immunogenic activity derives from the fungus and not the plant-based growth medium (Fig. S2e).

Because *F. oxysporum* infects Arabidopsis via the roots and plant organs or tissues can vary in their responsiveness to different elicitors (Ranf *et al.*, 2011), we tested organ-specific responses to EnFOE and compared these with responses to other fungal elicitors. We included chitin as a potent elicitor of root PTI responses, as well as the 23-AA Nep1-like peptide sequence from *F. oxysporum* (FoNLP) (Boehm *et al.*, 2014). Although both roots and shoots are responsive, EnFOE-triggered $[Ca^{2+}]_{cyt}$ elevations were higher in roots than in shoots. This was similar to the chitin response and in contrast to the FoNLP response, which was hardly detectable in roots (Fig. S3a–f). Weak PTI responses of roots also were reported for bacterial peptide elicitors *elf18* and *flg22*, which are detected predominantly in aboveground tissues (Ranf *et al.*, 2011). $[Ca^{2+}]_{cyt}$ elevations in response to *nlp20* were exclusively detected in the meristematic zone of the root (Wan *et al.*, 2018), which could explain the low responsiveness to FoNLP observed in root tissues. Taken together, these data confirm that PTI responses to EnFOE are strongest in the root and may therefore be spatially relevant for basal resistance against *F. oxysporum*.

Arabidopsis responses to EnFOE are partially dependent on known PTI signaling components and are suppressed by an effector from *Fusarium oxysporum*

In order to determine whether known PTI components are necessary for recognition of EnFOE, we monitored EnFOE-induced PTI responses in a range of PTI-signaling mutants. PTI responses to EnFOE were found to be independent of SUPPRESSOR OF BIR1 (SOBIR1; a core component of receptor complexes containing receptor-like proteins (Liebrand *et al.*, 2014)) and of CERK1, as shown previously for FOE (Figs 1b, 2a). BOTRYTIS-INDUCED KINASE 1 (BIK1) and PBS1-LIKE 1 (PBL1), cytoplasmic kinases involved in many PTI pathways (Ranf *et al.*, 2014), and the ROS-producing NADPH oxidase RESPIRATORY BURST OXIDASE HOMOLOG PROTEIN D (RBOHD) are required for full ROS responses to EnFOE (Fig. 2a). Hence, there is overlap in signaling components required for responses to EnFOE with those described for other elicitors.

The receptor-like kinase SOMATIC EMBRYOGENESIS RECEPTOR KINASE 3 (SERK3), also known as BAK1, is a central regulator of plant immune responses to immunogenic peptides and associates with multiple PRRs to initiate signal transduction in a partially redundant manner with other SERK-family proteins (Chinchilla *et al.*, 2007; Liebrand *et al.*, 2014). EnFOE-induced ROS production was reduced in *bak1-4* compared to WT plants suggesting that BAK1 is involved in EnFOE-triggered immune signaling (Fig. 2b,d). Mutants representing additional SERK proteins (a family of five leucine-rich repeat receptor-like protein kinases (LRR-RLKs) in Arabidopsis) with documented roles in cell-surface signaling pathways did not show

a significant reduction in EnFOE responsiveness (Fig. 2b). To further test for recognition of EnFOE by known PRRs, we measured EnFOE responses in additional mutant lines representing RECEPTOR-LIKE PROTEIN (RLP) 23, RLP30 and RLP42, each involved in detection of fungal elicitors (Zhang *et al.*, 2013, 2014; Albert *et al.*, 2015), or RESISTANCE TO FUSARIUM OXYSPORUM (RFO) 1, RFO2 and RFO3, known to be involved in quantitative resistance to *F. oxysporum* in Arabidopsis (de Sain & Rep, 2015). In each of these mutant lines, WT-like ROS responses were observed (Fig. 2c). Together, this suggested that our *Fusarium* elicitor preparations contain an unidentified elicitor that triggers canonical PTI responses in Arabidopsis.

In order to determine the potential biological relevance of EnFOE-mediated PTI in Arabidopsis–*Fusarium* interactions, we tested whether an effector from an adapted *F. oxysporum* strain is able to target EnFOE-mediated PTI responses. The *F. oxysporum* effector protein Avr2 functions as a virulence factor by suppressing PTI including *flg22*-induced responses (Di *et al.*, 2017). Two independent Arabidopsis lines stably expressing Avr2 lacking its signal peptide (*ΔspAVR2*) were severely impaired in ROS responses to EnFOE (Fig. 2e). These lines show a mild growth phenotype (Di *et al.*, 2017). *F. oxysporum* therefore produces an effector protein that can partially suppress PTI responses to an elicitor fraction derived from itself and subverting these responses might be relevant for establishing pathogenesis.

Forward genetics identified the *fusarium elicitor reduced elicitation 1* mutant

As forward genetic approaches do not require the molecular identity of the elicitor, we generated and screened Arabidopsis (Col-0^{AEQ}) EMS populations for attenuated $[Ca^{2+}]_{cyt}$ responses to FGE following protocols successfully used for isolating PTI-associated mutants (Ranf *et al.*, 2015). We focused on mutants with strongly reduced responses to FGE but largely unaltered responses to chitin and *flg22*. This identified a mutant, which we termed *fer1*, with partially reduced responses to crude FGE and FOE fractions, genetically supporting the presence of similar elicitor activity in different *Fusarium* species (Fig. S4a,b). This activity also was present in an elicitor preparation from *F. oxysporum* culture filtrate (Fig. S4c). EnFOE-induced PTI responses are abolished in *fer1* showing that we successfully enriched the relevant immunogenic fraction of FOE (Fig. 3a,b). We further confirmed that *fer1* is able to respond to the fungal elicitors chitin and FoNLP, to which WT-like or slightly enhanced responses were observed, suggesting specificity for EnFOE-induced PTI (Fig. 3c).

The gene underlying the *fer1* phenotype encodes the receptor-like kinase MIK2

In order to identify the causal mutation in *fer1*, we generated a *fer1* outcross population with ecotype Ler-0 and confirmed phenotypic segregation of a single recessive locus which we mapped subsequently using insertion/deletion markers (Salathia *et al.*, 2007). The mapping interval

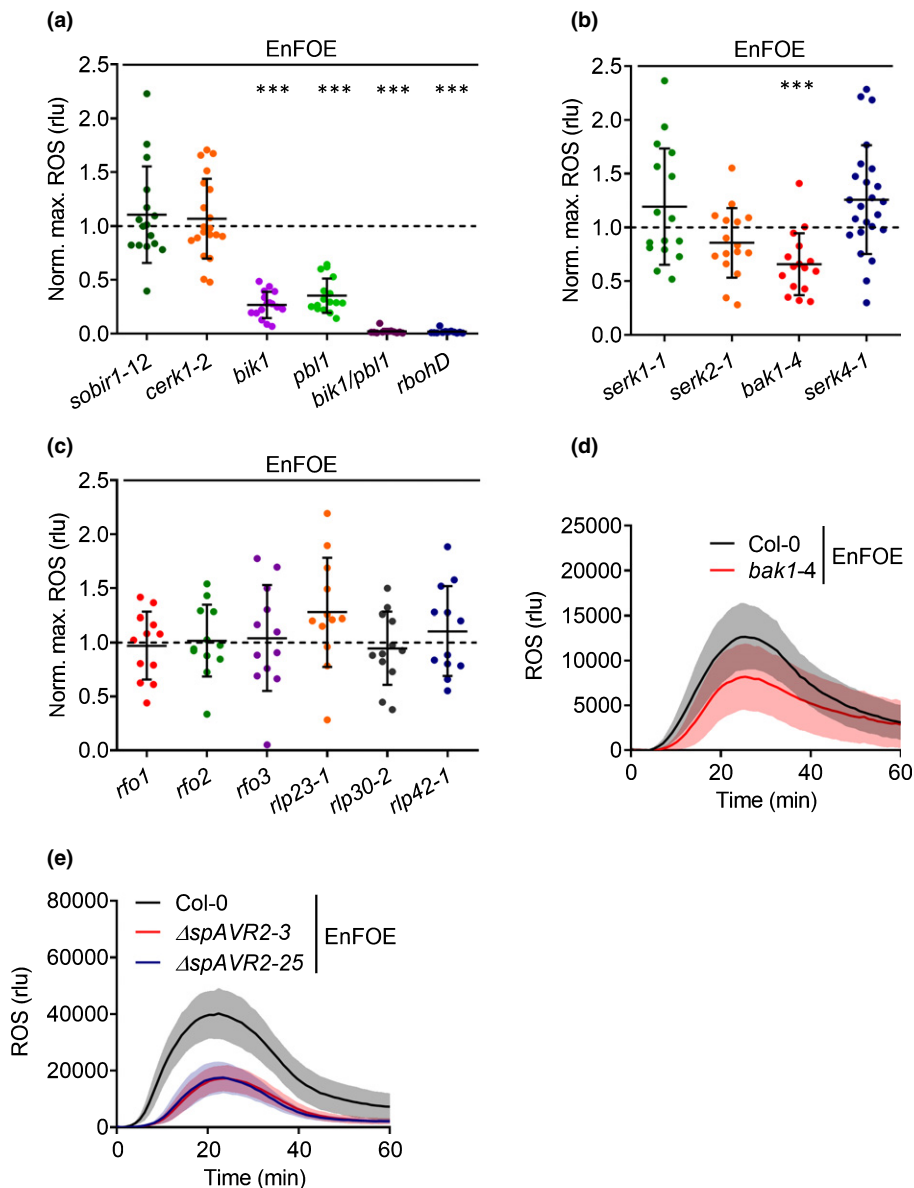


Fig. 2 Reactive oxygen species (ROS) response measurements in pattern-triggered immunity (PTI)-relevant *Arabidopsis thaliana* mutant genotypes. (a–c) Maximum ROS accumulation (in relative light units; rlu) measured in individual leaf discs (each plotted point) of various PTI-relevant mutant genotypes over 60 min after elicitation with enriched *Fusarium oxysporum* elicitor (EnFOE; $0.5 \mu\text{g ml}^{-1}$) normalized to the mean maxima of wild-type (WT) plants (set at 1; dashed line) \pm SD (a: $n = 16, 20, 16, 16, 12, 12$; b: $n = 16, 16, 16, 16$; c: $n = 12, 12, 12, 12, 12, 12$; left to right). (d) ROS accumulation kinetics in Col-0 and *bak1-4* leaf discs after elicitation with EnFOE ($0.5 \mu\text{g ml}^{-1}$). Data represent mean rlu measured from individual leaf discs \pm SD at each time point ($n = 16$). (e) ROS accumulation kinetics in Col-0 or stable *Arabidopsis* lines expressing the Avr2 effector from *F. oxysporum* lacking its signal peptide (ΔspAVR2) after elicitation with EnFOE ($0.5 \mu\text{g ml}^{-1}$). Data represent mean rlu measured from individual leaf discs \pm SD at each time point ($n = 12$). Data shown are normalized pooled data from multiple independent experiments (a: 4, 5, 4, 4, 3, 3; left to right; b: 4; c: 3), or pooled data from multiple independent experiments (d: 4; e: 3). Asterisks indicate significant differences (unpaired Student's *t*-test: ***, $P < 0.001$) compared to the WT control (Col-0).

contained a gene for an LRR-RLK called MIK2 (MALE DISCOVERER 1 (MDIS1)-INTERACTING RECEPTOR LIKE KINASE 2; also known as LRR-KISS). Because *MIK2* was the only gene in the mapping interval that encodes an obvious candidate PRR complex component by protein domain architecture, we sequenced *MIK2* in *fer1* and identified a single-nucleotide polymorphism (SNP) resulting in a premature W876STOP codon within the cytoplasmic kinase

domain. A gene model representing the *fer1* SNP and various *mik2* T-DNA insertion alleles used in this study is shown in Fig. 4(a). *MIK2* is a class XIIb LRR-RLK with described roles in cell-wall integrity sensing, root growth, sexual reproduction, and response to abiotic and biotic stress (Julkowska *et al.*, 2016; Wang *et al.*, 2016; Van der Does *et al.*, 2017). *MIK2* has one intron and the pre-mRNA is spliced into two forms (both of which are affected by the

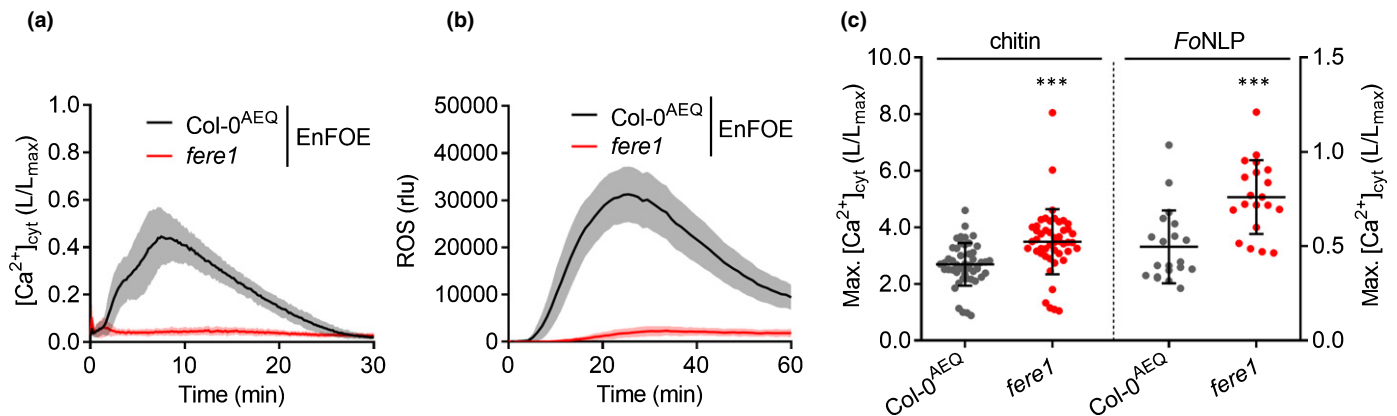


Fig. 3 Pattern-triggered immunity (PTI) marker responses in *fusarium elicitor reduced elicitation* (*fere1*) plants to fungal elicitors. (a) Cytosolic elevation of calcium ion concentration ($[Ca^{2+}]_{\text{cyt}}$) kinetics in Col-0^{Aeq} or *fere1* *Arabidopsis thaliana* seedlings after elicitation with enriched *Fusarium oxysporum* elicitor (EnFOE; $0.5 \mu\text{g ml}^{-1}$). Data represent mean values measured in individual seedlings \pm SD at each time point ($n = 40$). (b) Reactive oxygen species (ROS) accumulation kinetics in Col-0^{Aeq} or *fere1* leaf discs after elicitation with EnFOE ($0.5 \mu\text{g ml}^{-1}$). Data represent mean relative light units (rlu) measured from individual leaf discs \pm SD at each time point ($n = 12$). (c) Maximum $[Ca^{2+}]_{\text{cyt}}$ measured in individual Col-0^{Aeq} or *fere1* seedlings (each plotted point) over 30 min after elicitation with chitin ($75 \mu\text{g ml}^{-1}$; left y-axis) or FoNLP ($1 \mu\text{M}$; right y-axis) \pm SD ($n = 44, 44, 20, 20$; left to right). Data shown are pooled from multiple independent experiments (a: 6; b: 3; c: 8 for chitin, 4 for FoNLP). Asterisks indicate significant differences (unpaired *t*-test: ***, $P < 0.001$) compared to the wild-type (WT) control (Col-0^{Aeq}).

mutation in *fere1*, with splice variant *MIK2.1* being ≤ 50 -fold more abundant than *MIK2.2* (Van der Does *et al.*, 2017).

In order to gain evidence that the *fere1* SNP caused the loss of *Fusarium* elicitor responses, we tested T-DNA insertion lines with impaired MIK2 function (Alonso *et al.*, 2003; Rosso *et al.*, 2003). Three independent *mik2* alleles showed largely abolished PTI responses to EnFOE, but not to chitin to which a slightly enhanced ROS response was seen (Fig. 4b). In addition, we generated *mik2-3* mutants carrying the apoaequorin reporter (*mik2-3*^{Aeq}) and observed a similar loss-of-function phenotype in response to EnFOE as shown for *fere1* (Fig. 4c). Finally, the PTI loss-of-function phenotype in *fere1* to EnFOE was fully complemented by stable *MIK2* expression under the control of its own putative promoter as shown by ROS and $[Ca^{2+}]_{\text{cyt}}$ response measurements. Likewise this was achieved by using the predominant *MIK2.1* splice form amplified from cDNA in its native form (i.e. untagged), as well as the full-length genomic region of *MIK2* with a C-terminal cMyc peptide fusion (Figs 4d,e, S5). Bioassays performed with these lines indicated that *fere1* is more susceptible to *F. oxysporum* whereas WT-level resistance was restored in *MIK2*-complemented lines (Fig. S6). Together these data demonstrate that a *MIK2* loss-of-function underlies the *fere1* phenotype and that *MIK2* is essential for EnFOE-induced PTI responses.

MIK2-dependent elicitor activity is not restricted to the *Fusarium* genus

The strong PTI loss-of-function phenotype of *mik2* mutants to EnFOE can be used to genetically verify whether *MIK2*-dependent elicitor activity is present in other fungal species. To determine whether a conserved elicitor activity is present outside of the *Fusarium* genus, a comparable elicitor enrichment procedure

was performed for *Trichoderma atroviride* (EnTAE). *Trichoderma* is a fungal genus from the same order (*Hypocreales* within the class of *Sordariomycetes*) as *Fusarium* (Crous *et al.*, 2004). EnTAE gave a strong ROS response in WT plants, which was severely impaired in the three independent *mik2* T-DNA mutants (Fig. S7a). Similar to EnFOE, ROS responses to EnTAE were independent of CERK1, yet partially or fully dependent on BAK1, BIK1, PBL1 and RBOHD (Figs S7a, 2a). The EnTAE-induced ROS response was reduced in *fere1* plants yet fully restored in *fere1/MIK2* complementation lines, confirming that *MIK2* also is essential for PTI responses to EnTAE (Fig. S7b,c). Together, these data show that *MIK2*-dependent elicitor activity also is present in fungi closely related to *Fusarium*.

FERONIA is required for the full response to EnFOE

So far, *MIK2* has not been implicated in PTI responses, but its expression is affected by pathogen infection or elicitor treatment (based on the *Arabidopsis* eFP Browser (Winter *et al.*, 2007); Expression sets 1007966202 and 1008080727). Notably, *MIK2* is important for resistance against *F. oxysporum* which previously was linked to its role in cell-wall integrity (CWI) monitoring (Van der Does *et al.*, 2017). Our data suggest that the additional role of *MIK2* in EnFOE-triggered PTI also could contribute to this resistance. PTI and CWI sensing are intimately interconnected (Hamann, 2012; Wolf, 2017; Engelsdorf *et al.*, 2018), and it has been reported that *mik2* shows reduced defence activation following isoxaben-induced inhibition of cellulose biosynthesis (Van der Does *et al.*, 2017; Engelsdorf *et al.*, 2018). To determine whether CWI sensing generally interferes with EnFOE sensing, we tested EnFOE responsiveness in mutant genotypes representing cell-surface RLKs with known roles in CWI sensing (e.g. HERCULES 1 (*herk1*), WALL-ASSOCIATED KINASE 2 (*wak2*), and

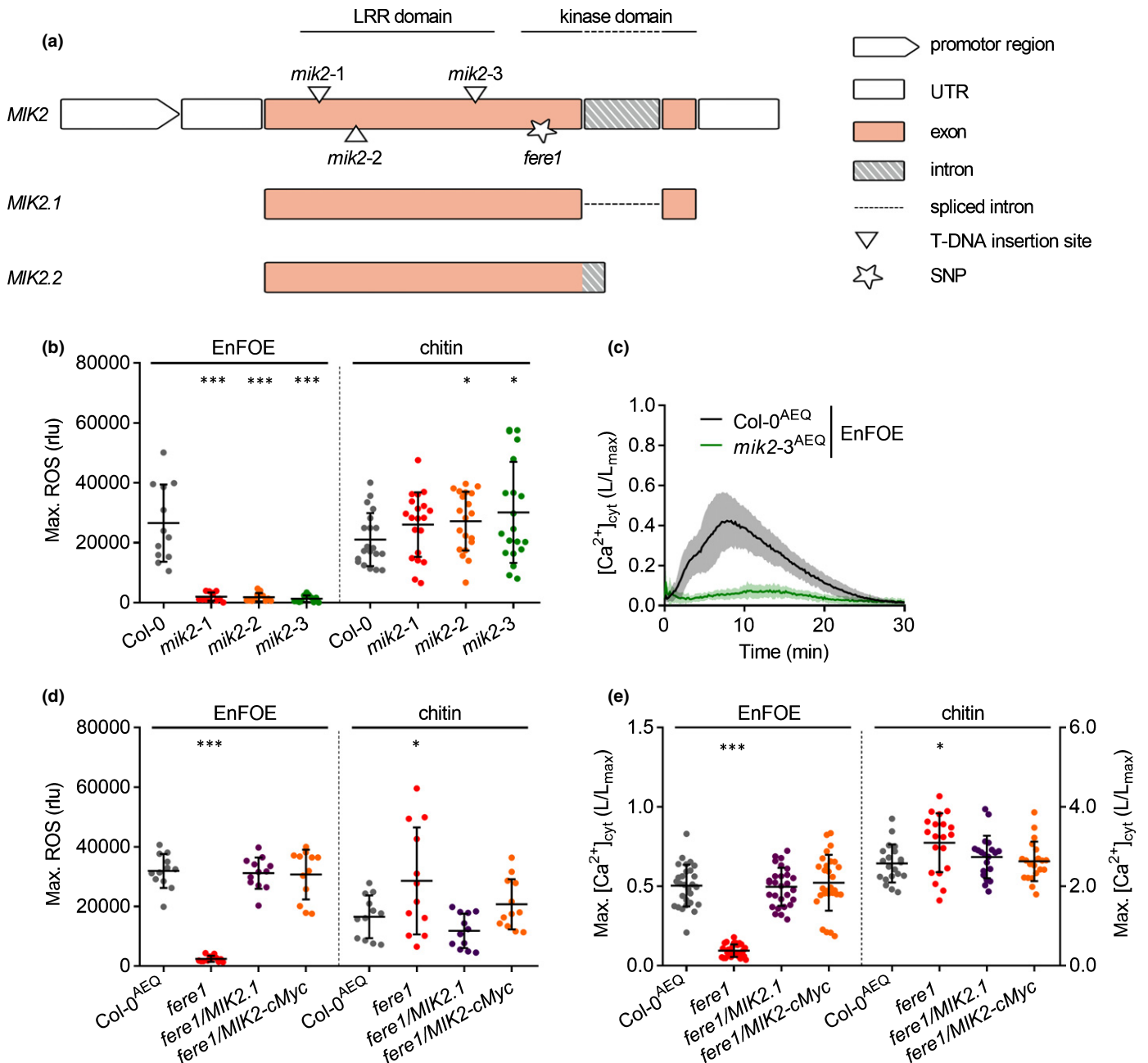


Fig. 4 Pattern-triggered immunity (PTI) marker responses in various *mik2* alleles and MDIS1-INTERACTING RECEPTOR-LIKE KINASE 2 (MIK2)-complemented *Arabidopsis thaliana* plants to fungal elicitors. (a) *MIK2* gene model showing predicted splice forms (*MIK2.1*, *MIK2.2*) and locations of the *fusarium elicitor reduced elicitation1* (*fere1*) single nucleotide polymorphism (SNP) or relevant T-DNA insertions. (b) Maximum reactive oxygen species (ROS) accumulation (in relative light units; rlu) measured in individual leaf discs (each plotted point) from Col-0 or three independent *mik2* T-DNA mutants over 60 min after elicitation with enriched *Fusarium oxysporum* elicitor (EnFOE; 0.5 µg ml⁻¹) or chitin (75 µg ml⁻¹) ± SD (*n* = 12, 12, 12, 12, 20, 20, 20, 20; left to right). (c) Cytosolic elevation of calcium ion concentration ([Ca²⁺]_{cyt}) kinetics in Col-0^{AEO} or *mik2-3*^{AEO} seedlings after elicitation with EnFOE (0.5 µg ml⁻¹). Data represent mean values measured in individual leaf discs ± SD at each time point (*n* = 24). (d) Maximum ROS accumulation (rlu) measured in individual leaf discs (each plotted point) from Col-0^{AEO}, *fere1*, *fere1/MIK2.1* or *fere1/MIK2-cMyc* over 60 min after elicitation with EnFOE (0.5 µg ml⁻¹) or chitin (75 µg ml⁻¹) ± SD (*n* = 12, 12, 12, 12, 12, 12, 12, 12; left to right). (e) Maximum [Ca²⁺]_{cyt} measured in individual Col-0^{AEO}, *fere1*, *fere1/MIK2.1* or *fere1/MIK2-cMyc* seedlings (each plotted point) over 30 min after elicitation with EnFOE (0.5 µg ml⁻¹; left y-axis) or chitin (75 µg ml⁻¹; right y-axis) ± SD (*n* = 28, 28, 28, 28, 20, 20, 20, 20; left to right). Data shown are pooled from multiple independent experiments (b: 3 for EnFOE, 5 for chitin; c: 5; d: 3; e: 5 for EnFOE, 4 for chitin). Asterisks indicate significant difference (unpaired Student's *t*-test: *, *P* < 0.05; ***, *P* < 0.001) compared to the respective wild-type (WT) control (Col-0 or Col-0^{AEO}).

THESEUS 1 (*the1*) (Engelsdorf *et al.*, 2018). A WT-like ROS response was observed in *herk1*, *wak2*, and two independent *the1* alleles (*the1-1* [null mutant] and *the1-4* [reported to

be hypermorphic (Merz *et al.*, 2017)]) to EnFOE (Fig. S8a), showing that impairment in CWI sensing generally does not interfere with EnFOE responses.

Interestingly, a markedly reduced EnFOE-induced ROS response was observed in *FERONIA fer-4* mutants and *llg1-2* mutants (LORELEI-LIKE GPI ANCHORED PROTEIN 1; a chaperone of *FERONIA* involved in perception of RAPID ALKALINIZATION FACTOR (RALF) peptides and receptor complex assembly) (Fig. S8c–e), indicating a role of *FERONIA* in EnFOE-induced PTI signaling consistent with its role in controlling various immune signaling processes (Li *et al.*, 2015; Shen *et al.*, 2017; Stegmann *et al.*, 2017; Xiao *et al.*, 2019). WT-like responses to Pep1, an endogenous 23-AA damage-associated peptide recognized by LRR-RLKs PEPR1 and PEPR2 (PERCEPTION OF THE ARABIDOPSIS DANGER SIGNAL PEPTIDE 1/2) in Arabidopsis (Yamaguchi *et al.*, 2010), were observed in *fer-4* and *llg1-2* mutants however. As *FERONIA* and *LLG1* are required for full EnFOE-induced PTI responses and *Fusarium* spp. such as *F. oxysporum* are known to secrete functional plant RALF homologs as pathogenicity factors (Masachis *et al.*, 2016), we speculated whether *MIK2* was involved in responses to RALF peptides. ROS production upon treatment with a synthetic RALF17 peptide was not impaired in *mik2-3* whereas *llg1-2* and *fer-4* were completely insensitive, suggesting that *MIK2* is not directly involved in responses to a PTI-inducing RALF peptide (Fig. S8f).

MIK2 has a close homolog (60% AA identity) termed *MIK2-LIKE* which may have genetic relatedness to *MIK2* in the context of CWI monitoring via control of root growth angle, yet seemingly does not fulfil the same function as *MIK2* in responses to cellulose-biosynthesis inhibition (Van der Does *et al.*, 2017). Although the strong loss-of-function phenotype of *fer1* and other *mik2* alleles in response to EnFOE argues against redundancy of this response, we tested two independent *mik2-like* T-DNA insertion mutants for EnFOE-induced PTI responses. The *mik2-like* mutant plants did not show a reduced ROS response to EnFOE (Fig. S8b), whereas *mik2/mik2-like* double mutants showed a loss-of-function phenotype consistent with loss-of-function *MIK2*. Taken together, these data suggest that failure in CWI sensing does not generally interfere with Arabidopsis

responses to EnFOE, but *FERONIA* and *LLG1* contribute to full sensitivity.

Ectopic expression of *AtMIK2* in *Nicotiana benthamiana* confers sensitivity to EnFOE

As EnFOE did not trigger ROS production in leaf discs from solanaceous *N. benthamiana* plants (Fig. S1), we investigated whether transient expression of Arabidopsis *MIK2* could confer sensitivity to EnFOE. Indeed, a rapid production of ROS in *N. benthamiana* leaf discs after elicitation with EnFOE was observed upon heterologous expression of functional *AtMIK2*, but not a kinase-dead variant or the truncated *FERE1* variant (Figs 5a,b, S9). This indicates that the *AtMIK2* protein is sufficient to confer sensitivity to EnFOE and its kinase domain is essential for EnFOE-induced signaling in *N. benthamiana*. Notably, we found that *BAK1* weakly associates with *MIK2* when co-expressed in *N. benthamiana* and that this association is enforced upon EnFOE application (Fig. S10).

Discussion

Considering that fungi represent ubiquitous phytopathogens, it is likely that plants are capable of recognizing many immunogenic patterns from these organisms via a diverse assortment of cell-surface receptors. The Arabidopsis genome alone encodes over 400 receptor-like kinases (RLKs) with a predicted extracellular domain and only a small fraction of these have a demonstrated biological role (Shiu & Bleecker, 2001). We therefore sought potential pattern-triggered immunity (PTI) components to *Fusarium* extracts that could be underlying quantitative resistance and identified *MDIS1-INTERACTING RECEPTOR-LIKE KINASE 2* (*MIK2*) as a key module in *Fusarium* sensing. Although we have not yet identified the elicitor, the finding that *MIK2*-dependent elicitor activity is present in diverse *Fusarium* spp. and the related *Trichoderma atroviride* suggests that *MIK2* is key to detection of a conserved molecular pattern.

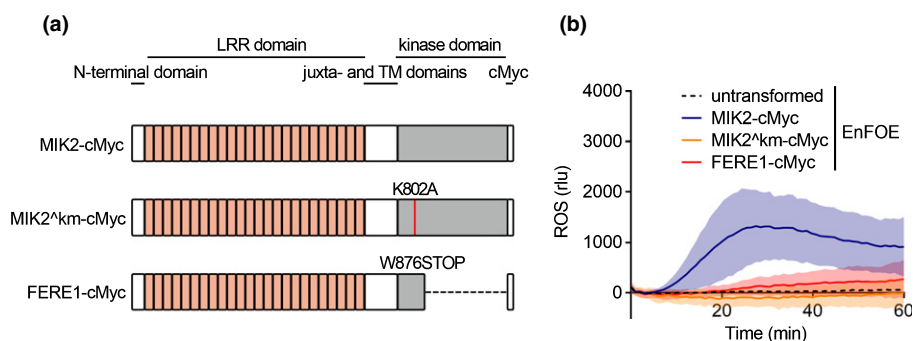


Fig. 5 Transient expression of *Arabidopsis thaliana* MDIS1-INTERACTING RECEPTOR-LIKE KINASE 2 (*MIK2*) protein variants in *Nicotiana benthamiana*. (a) Protein model of *MIK2* variants showing relevant domains (LRR, leucine-rich repeat; TM, transmembrane). (b) Reactive oxygen species (ROS) accumulation kinetics in leaf discs from *N. benthamiana* either untransformed or transiently transformed with Arabidopsis wild-type (WT) *MIK2*-cMyc, the truncated *FUSARIUM ELICITOR REDUCED ELICITATION 1* (*FERE1*)-cMyc variant, or a kinase dead variant (*MIK2*^{km}-cMyc) after elicitation with EnFOE ($2 \mu\text{g ml}^{-1}$). Data represent mean relative light units (rlu) measured from individual leaf discs \pm SD at each measurement point ($n = 20$). ROS kinetics indicated with a dashed line are shown without SD for clarity. Data shown are pooled from multiple independent experiments ($b: 3$).

Enriched *Fusarium oxysporum* elicitor (EnFOE)-mediated responses in Arabidopsis are dependent on several components previously implicated in PTI pathways and are suppressed by the *F. oxysporum* effector protein Avr2. Although the precise target of Avr2 is not yet known, the general PTI-suppressive capacity of Avr2 (Di *et al.*, 2017) provides further evidence that EnFOE-mediated signaling converges into common PTI pathways and could therefore contribute to basal resistance. We could confirm that *fusarium elicitor reduced elicitation 1 (fere1)* is more susceptible to *F. oxysporum* as shown previously for *mik2* T-DNA mutant lines (Van der Does *et al.*, 2017) and further demonstrated that the reduced resistance could be complemented by *MIK2* expression. The relative contribution of EnFOE-mediated PTI in quantitative resistance against *Fusarium* spp., or to other fungi with *MIK2*-dependent elicitor activity, remains a topic for future studies. However, the current lack of a purified elicitor and confounding effects of *MIK2* function in biological processes other than susceptibility might complicate these studies.

The full extent of *MIK2* function in PTI and how this relates to its other described roles remains an open question. *MIK2* domain architecture is similar to class XIIa LRR-RLK members FLAGELLIN-SENSITIVE 2 (FLS2) and EF-Tu RECEPTOR (EFR), which are *bona fide* PRRs, yet the involvement of *MIK2* in cell wall integrity (CWI) sensing and salt tolerance (Julkowska *et al.*, 2016; Van der Does *et al.*, 2017; Engelsdorf *et al.*, 2018) suggests that it may be involved in perception of both endogenous and exogenous signals. This does not exclude that *MIK2* also could function as a direct peptide receptor. Indeed, the almost complete loss-of-function phenotype in diverse *mik2* alleles to EnFOE indicates a key role in elicitor perception. Comparably, the RLK FERONIA, which has multiple functions in plants, also was shown to be a receptor for RALF peptides (Stegmann *et al.*, 2017). The plant response to EnFOE is rapid and within the time frame of directly-perceived elicitors such as *flg22* (Chinchilla *et al.*, 2007). Therefore, direct binding of the elicitor is a likely explanation yet we cannot fully exclude something is released from the plant upon elicitor treatment (i.e. a damage-associated molecular pattern (DAMP)), which then triggers the observed responses. Residual enzymatic activity in EnFOE appears unlikely, however, because the extracts have been autoclaved before elicitor enrichment. Additionally, *Nicotiana benthamiana* would have to release a similar plant signal without having the corresponding *MIK2*-dependent response. Together with the ability of *MIK2* to confer EnFOE sensitivity to *N. benthamiana*, this argues for *MIK2* being a key part of plant recognition machinery that directly interacts with EnFOE. This hypothesis is further supported by the enhanced association of BAK1 with *MIK2* in *N. benthamiana* after application of EnFOE, which is reminiscent of ligand-dependent receptor-complex formation (Chinchilla *et al.*, 2007). Considering its involvement in responses to internal and external stimuli, *MIK2* might therefore be an integrator of diverse signals for coordinated plant response to the environment.

Determining the presence of *MIK2*-dependent elicitor activity in diverse fungal species may greatly widen the role of *MIK2* not only in resistance against fungal pathogens, but also to

interactions with endophytic and beneficial fungi. *Fusarium* and *Trichoderma* spp. are common in soil and root ecosystems, and also can act as opportunistic plant symbionts that penetrate into the root epidermis and outer cortex to establish a long-term, robust colonization (Harman *et al.*, 2004; Bacon & Yates, 2006). *MIK2* could therefore modulate root colonization via perception of EnFOE-like elicitor activity from these fungi. Conserved elicitors from both pathogenic and commensal fungi can be equally perceived by plants and trigger PTI responses. However, mechanisms by which root systems initiate localized PTI responses at sites of pathogen attack without endangering commensal microbes have been demonstrated recently (Zhou *et al.*, 2020). It will therefore be interesting to examine the role of *MIK2* and *MIK2*-dependent PTI at local sites of root colonization by both pathogenic and commensal fungi.

Molecular identification of EnFOE is an important target for future work. However, elicitor identification has proven challenging in some cases (e.g. for *Sclerotinia* culture filtrate elicitor 1 or enigmatic MAMP of *Xanthomonas*) (Jehle *et al.*, 2013; Zhang *et al.*, 2013). Genetic resources can greatly assist elicitor characterization. For example, the LIPOOLIGOSACCHARIDE-SPECIFIC REDUCED ELICITATION (LORE) receptor mutant was crucial for further chemical dissection of the plant PTI response to enriched lipopolysaccharide fractions from *Pseudomonas* species and guided the identification of medium chain length 3-hydroxy fatty acids as the actual bacterial elicitors (Kutschera *et al.*, 2019). Similar approaches with *MIK2* could be used to guide EnFOE identification. Moreover, physical and/or genetic interaction studies with *MIK2* may disclose the nature of the PRR complex responsible for PTI responses to EnFOE.

Alongside *MIK2*, several other LRR-containing cell-surface receptors have been recognized to contribute towards resistance against *Fusarium* spp. in plants, including homologous LRR-RLK genes from barley (*HvLRRK-6H*) and wheat (*TaLRRK-6D*) which contribute to basal defense against *Fusarium* head blight (Thapa *et al.*, 2018), and Arabidopsis *RFO2* and tomato *I-7* genes which encode receptor-like proteins involved in *Fusarium* wilt resistance (Shen & Diener, 2013; Gonzalez-Cendales *et al.*, 2016). Fundamental research in the model Arabidopsis will accelerate the process of identifying additional cell-surface receptors and downstream PTI components in crop plants, where *Fusarium* species cause relevant yield losses but comparable genetic resources are currently unavailable. *MIK2* has putative orthologs of unknown function in several crop species, which may allow for comparative genomics between model and crop towards improved *Fusarium*-resistance breeding. Future genetic studies can be used to validate whether the PTI responses that we observe in soybean and barley to EnFOE correspond to a conserved recognition mechanism or to species-specific sensing of additional elicitors present in our enrichments. Finally, there are several examples of successful transfer of PRRs to enhance disease resistance (Boutrot & Zipfel, 2017; Ranf, 2018). PRRs or other components found in Arabidopsis might be transferred to crops or recombined with crop genes to link up with endogenous immune components and thereby engineer durable and broad-spectrum resistance.


Acknowledgements


This work was supported by the BASF Plant Science Company GmbH (R&D cooperation with SR and RH) and a grant from the German Research Foundation to RH (HU886/11). FLWT is supported by NWO-funded VICI project no. 865.14.00 and SR by DFG Emmy Noether program RA2541/1. We are grateful to Holger Schultheiss (BASF Plant Science Company GmbH) and Martin Stegmann (Phytopathology, TU Munich) for fruitful discussions.


Author contributions


RH and SR designed the study; SR, RH, FLWT, ADC and JM planned the experiments and interpreted results; ADC, JM and LR optimized methodology and performed experiments; ADC and JM prepared figures; and ADC and RH wrote and revised the manuscript. All authors discussed and approved the final manuscript.


ORCID

Alexander D. Coleman  <https://orcid.org/0000-0001-7771-2290>

Ralph Hüchelhoven  <https://orcid.org/0000-0001-5632-5451>

Julian Maroschek  <https://orcid.org/0000-0003-2451-050X>

Stefanie Ranf  <https://orcid.org/0000-0003-2262-2938>

Frank L.W. Takken  <https://orcid.org/0000-0003-2655-3108>

References

- Albert I, Bohm H, Albert M, Feiler CE, Imkamp J, Wallmeroth N, Brancato C, Raaymakers TM, Oome S, Zhang HQ *et al.* 2015. An RLP23-SOBIR1-BAK1 complex mediates NLP-triggered immunity. *Nature Plants* 1: 9.
- Alonso JM, Stepanova AN, Leisse TJ, Kim CJ, Chen HM, Shinn P, Stevenson DK, Zimmerman J, Barajas P, Cheuk R *et al.* 2003. Genome-wide Insertional mutagenesis of *Arabidopsis thaliana*. *Science* 301: 653–657.
- Bacon CW, Yates IE. 2006. Endophytic root colonization by *Fusarium* Species: Histology, plant interactions, and toxicity. In Schulz BJE, Boyle CJC, Sieber TN, eds. *Microbial root endophytes*. Berlin: Springer, 133–152.
- Boehm H, Albert I, Oome S, Raaymakers TM, Van den Ackerveken G, Nuernberger T. 2014. A conserved peptide pattern from a widespread microbial virulence factor triggers pattern-induced immunity in *Arabidopsis*. *PLoS Pathogens* 10: e1004491.
- Boller T, Felix G. 2009. A renaissance of elicitors: Perception of microbe-associated molecular patterns and danger signals by pattern-recognition receptors. *Annual Review of Plant Biology* 60: 379–406.
- Boutrot F, Zipfel C. 2017. Function, discovery, and exploitation of plant pattern recognition receptors for broad-spectrum disease resistance. *Annual Review of Phytopathology* 55: 257–286.
- Chinchilla D, Zipfel C, Robatzek S, Kemmerling B, Nuernberger T, Jones JDG, Felix G, Boller T. 2007. A flagellin-induced complex of the receptor FLS2 and BAK1 initiates plant defence. *Nature* 448: 497–500.
- Chivasa S, Simon WJ, Yu X-L, Yalpani N, Slabas AR. 2005. Pathogen elicitor-induced changes in the maize extracellular matrix proteome. *Proteomics* 5: 4894–4904.
- Couto D, Zipfel C. 2016. Regulation of pattern recognition receptor signalling in plants. *Nature Reviews Immunology* 16: 537–552.
- Crous PW, Gams W, Stalpers JA, Robert V, Stegehuis G. 2004. MycoBank: an online initiative to launch mycology into the 21st century. *Studies in Mycology* 50: 19–22.
- Dale J, James A, Paul J-Y, Khanna H, Smith M, Peraza-Echeverria S, Garcia-Bastidas F, Kema G, Waterhouse P, Mengersen K *et al.* 2017. Transgenic Cavendish bananas with resistance to Fusarium wilt tropical race 4. *Nature Communications* 8: 1496.
- Davies DR, Bindschedler LV, Strickland TS, Bolwell GP. 2006. Production of reactive oxygen species in *Arabidopsis thaliana* cell suspension cultures in response to an elicitor from *Fusarium oxysporum*: implications for basal resistance. *Journal of Experimental Botany* 57: 1817–1827.
- Dey S, Ghose K, Basu D. 2009. Fusarium elicitor-dependent calcium influx and associated ROS generation in tomato is independent of cell death. *European Journal of Plant Pathology* 126: 217.
- Di X, Cao L, Hughes RK, Tintor N, Banfield MJ, Takken FLW. 2017. Structure-function analysis of the *Fusarium oxysporum* Avr2 effector allows uncoupling of its immune-suppressing activity from recognition. *New Phytologist* 216: 897–914.
- Dita M, Barquero M, Heck D, Mizubuti ESG, Staver CP. 2018. Fusarium wilt of banana: Current knowledge on epidemiology and research needs toward sustainable disease management. *Frontiers in Plant Science* 9: 1468.
- Engelsdorf T, Gigli-Bisceglia N, Veerabagu M, McKenna JF, Vaahtera L, Augstein F, Van der Does D, Zipfel C, Hamann T. 2018. The plant cell wall integrity maintenance and immune signaling systems cooperate to control stress responses in *Arabidopsis thaliana*. *Science Signaling* 11: eaao3070.
- Felix G, Duran JD, Volko S, Boller T. 1999. Plants have a sensitive perception system for the most conserved domain of bacterial flagellin. *The Plant Journal* 18: 265–276.
- Gomez-Gomez L, Boller T. 2000. FLS2: An LRR receptor-like kinase involved in the perception of the bacterial elicitor flagellin in *Arabidopsis*. *Molecular Cell* 5: 1003–1011.
- Gonzalez-Cendales Y, Catanzariti AM, Baker B, McGrath DJ, Jones DA. 2016. Identification of I-7 expands the repertoire of genes for resistance to Fusarium wilt in tomato to three resistance gene classes. *Molecular Plant Pathology* 17: 448–463.
- Gotthardt M, Kanawati B, Schmidt F, Asam S, Hammerl R, Frank O, Hofmann T, Schmitt-Kopplin P, Rychlik M. 2020. Comprehensive analysis of the *Alternaria* mycobiome using mass spectrometry based metabolomics. *Molecular Nutrition & Food Research* 64: 1900558.
- Hamann T. 2012. Plant cell wall integrity maintenance as an essential component of biotic stress response mechanisms. *Frontiers in Plant Science* 3: 77.
- Hao Y, Rasheed A, Zhu Z, Wulff BBH, He Z. 2020. Harnessing wheat Fhb1 for Fusarium resistance. *Trends in Plant Science* 25: 1–3.
- Harman GE, Howell CR, Viterbo A, Chet I, Lorito M. 2004. *Trichoderma* species – opportunistic, avirulent plant symbionts. *Nature Reviews Microbiology* 2: 43–56.
- Jehle AK, Lipschis M, Albert M, Fallahzadeh-Mamaghani V, Fuerst U, Mueller K, Felix G. 2013. The Receptor-Like Protein ReMAX of *Arabidopsis* detects the microbe-associated molecular pattern eMax from *Xanthomonas*. *Plant Cell* 25: 2330–2340.
- Julkowska MM, Klei K, Fokkens L, Haring MA, Schranz ME, Testerink C. 2016. Natural variation in rosette size under salt stress conditions corresponds to developmental differences between *Arabidopsis* accessions and allelic variation in the LRR-KISS gene. *Journal of Experimental Botany* 67: 2127–2138.
- Kesten C, Gámez-Arjona FM, Menna A, Scholl S, Dora S, Huerta AI, Huang H-Y, Tintor N, Kinoshita T, Rep M *et al.* 2019. Pathogen-induced pH changes regulate the growth-defense balance in plants. *EMBO Journal* 38: e101822.
- Knight MR, Campbell AK, Smith SM, Trewavas AJ. 1991. Transgenic plant aquorin reports the effects of touch and cold-shock and elicitors on cytoplasmic calcium. *Nature* 352: 524–526.
- Kutschera A, Dawid C, Gisch N, Schmid C, Raasch L, Gerster T, Schäffer M, Smakowska-Luzan E, Belkhadir Y, Vlot AC *et al.* 2019. Bacterial medium-chain 3-hydroxy fatty acid metabolites trigger immunity in *Arabidopsis* plants. *Science* 364: 178–181.

- Li C, Yeh FL, Cheung AY, Duan Q, Kita D, Liu MC, Maman J, Luu EJ, Wu BW, Gates L *et al.* 2015. Glycosylphosphatidylinositol-anchored proteins as chaperones and co-receptors for FERONIA receptor kinase signaling in Arabidopsis. *eLife* 4: e06587.
- Li S, Dong Y, Li L, Zhang Y, Yang X, Zeng H, Shi M, Pei X, Qiu D, Yuan Q. 2019a. The Novel Cerato-Platanin-Like Protein FocCP1 from *Fusarium oxysporum* triggers an immune response in plants. *International Journal of Molecular Sciences* 20: 2849.
- Li S, Nie H, Qiu D, Shi M, Yuan Q. 2019b. A novel protein elicitor PeFOC1 from *Fusarium oxysporum* triggers defense response and systemic resistance in tobacco. *Biochemical and Biophysical Research Communications* 514: 1074–1080.
- Liebrandt TWH, van den Burg HA, Joosten MHJ. 2014. Two for all: receptor-associated kinases SOBIR1 and BAK1. *Trends in Plant Science* 19: 123–132.
- Livak KJ, Schmittgen TD. 2001. Analysis of relative gene expression data using real-time quantitative PCR and the 2(T)(-Delta Delta C) method. *Methods* 25: 402–408.
- Masachis S, Segorbe D, Turra D, Leon-Ruiz M, Furst U, El Ghalid M, Leonard G, Lopez-Berges MS, Richards TA, Felix G *et al.* 2016. A fungal pathogen secretes plant alkalinizing peptides to increase infection. *Nature Microbiology* 1: 16043.
- McDonald BA, Linde C. 2002. Pathogen population genetics, evolutionary potential, and durable resistance. *Annual Review of Phytopathology* 40: 349–379.
- Merz D, Richter J, Gonneau M, Sanchez-Rodriguez C, Eder T, Sormani R, Martin M, Hématy K, Höfte H, Hauser M-T. 2017. T-DNA alleles of the receptor kinase THESEUS1 with opposing effects on cell wall integrity signaling. *Journal of Experimental Botany* 68: 4583–4593.
- Miya A, Albert P, Shinya T, Desaki Y, Ichimura K, Shirasu K, Narusaka Y, Kawakami N, Kaku H, Shibuya N. 2007. CERK1, a LysM receptor kinase, is essential for chitin elicitor signaling in Arabidopsis. *Proceedings of the National Academy of Sciences, USA* 104: 19613–19618.
- Ndimba BK, Chivasa S, Hamilton JM, Simon WJ, Slabas AR. 2003. Proteomic analysis of changes in the extracellular matrix of Arabidopsis cell suspension cultures induced by fungal elicitors. *Proteomics* 3: 1047–1059.
- Neff MM, Turk E, Kalishman M. 2002. Web-based primer design for single nucleotide polymorphism analysis. *Trends in Genetics* 18: 613–615.
- Oome S, Raaymakers TM, Cabral A, Samwel S, Bohm H, Albert I, Nurnberger T, Van den Ackerveken G. 2014. Nep1-like proteins from three kingdoms of life act as a microbe-associated molecular pattern in Arabidopsis. *Proceedings of the National Academy of Sciences, USA* 111: 16955–16960.
- Ranf S. 2018. Pattern recognition receptors versatile genetic tools for engineering broad-spectrum disease resistance in crops. *Agronomy* 8: 134.
- Ranf S, Eschen-Lippold L, Fröhlich K, Westphal L, Scheel D, Lee J. 2014. Microbe-associated molecular pattern-induced calcium signaling requires the receptor-like cytoplasmic kinases, PBL1 and BIK1. *BMC Plant Biology* 14: 374.
- Ranf S, Eschen-Lippold L, Pecher P, Lee J, Scheel D. 2011. Interplay between calcium signalling and early signalling elements during defence responses to microbe- or damage-associated molecular patterns. *The Plant Journal* 68: 100–113.
- Ranf S, Gisch N, Schaeffer M, Illig T, Westphal L, Knirel YA, Sanchez-Carballo PM, Zaehring U, Hueckelhoven R, Lee J *et al.* 2015. A lectin S-domain receptor kinase mediates lipopolysaccharide sensing in *Arabidopsis thaliana*. *Nature Immunology* 16: 426–433.
- Ranf S, Grimmer J, Poeschl Y, Pecher P, Chinchilla D, Scheel D, Lee J. 2012. Defense-related calcium signaling mutants uncovered via a quantitative high-throughput screen in *Arabidopsis thaliana*. *Molecular Plant* 5: 115–130.
- Ron M, Avni A. 2004. The receptor for the fungal elicitor ethylene-inducing xylanase is a member of a resistance-like gene family in tomato. *Plant Cell* 16: 1604–1615.
- Rosso MG, Li Y, Strizhov N, Reiss B, Dekker K, Weisshaar B. 2003. An *Arabidopsis thaliana* T-DNA mutagenized population (GABI-Kat) for flanking sequence tag-based reverse genetics. *Plant Molecular Biology* 53: 247–259.
- Saijo Y, Loo EP, Yasuda S. 2018. Pattern recognition receptors and signaling in plant-microbe interactions. *The Plant Journal* 93: 592–613.
- de Sain M, Rep M. 2015. The role of pathogen-secreted proteins in fungal vascular wilt diseases. *International Journal of Molecular Sciences* 16: 23970–23993.
- Salathia N, Lee HN, Sangster TA, Morneau K, Landry CR, Schellenberg K, Behere AS, Gunderson KL, Cavalieri D, Jander G *et al.* 2007. Indel arrays: an affordable alternative for genotyping. *The Plant Journal* 51: 727–737.
- Sanchez-Vallet A, Mesters JR, Thomma B. 2015. The battle for chitin recognition in plant-microbe interactions. *FEMS Microbiology Reviews* 39: 171–183.
- Shen QJ, Bourdais G, Pan HR, Robatzek S, Tang DZ. 2017. Arabidopsis glycosylphosphatidylinositol-anchored protein LLG1 associates with and modulates FLS2 to regulate innate immunity. *Proceedings of the National Academy of Sciences, USA* 114: 5749–5754.
- Shen Y, Diener AC. 2013. *Arabidopsis thaliana* RESISTANCE TO FUSARIUM OXYSPORUM 2 implicates tyrosine-sulfated peptide signaling in susceptibility and resistance to root infection. *PLoS Genetics* 9: e1003525.
- Shiu S-H, Bleeker AB. 2001. Receptor-like kinases from Arabidopsis form a monophyletic gene family related to animal receptor kinases. *Proceedings of the National Academy of Sciences, USA* 98: 10763–10768.
- Stegmann M, Monaghan J, Smakowska-Luzan E, Rovenich H, Lehner A, Holton N, Belkhadir Y, Zipfel C. 2017. The receptor kinase FER is a RALF-regulated scaffold controlling plant immune signaling. *Science* 355: 287–289.
- Thapa G, Gunupuru LR, Hehir JG, Kahla A, Mullins E, Doohan FM. 2018. A pathogen-responsive leucine rich receptor like kinase contributes to *Fusarium* resistance in cereals. *Frontiers in Plant Science* 9: 867.
- Van der Does D, Boutrot F, Engelsdorf T, Rhodes J, McKenna JF, Vernhettes S, Koevoets I, Tintor N, Veerabagu M, Miedes E *et al.* 2017. The Arabidopsis leucine-rich repeat receptor kinase MIK2/LRR-KISS connects cell wall integrity sensing, root growth and response to abiotic and biotic stresses. *PLoS Genetics* 13: e1006832.
- Wan WL, Zhang L, Pruitt R, Zaidem M, Brugman R, Ma X, Krol E, Perraki A, Kilian J, Grossmann G *et al.* 2018. Comparing Arabidopsis receptor kinase and receptor protein-mediated immune signaling reveals BIK1-dependent differences. *New Phytologist* 221: 2080–2095.
- Wang T, Liang L, Xue Y, Jia PF, Chen W, Zhang MX, Wang YC, Li HJ, Yang WC. 2016. A receptor heteromer mediates the male perception of female attractants in plants. *Nature* 531: 241–244.
- Winter D, Vinegar B, Nahal H, Ammar R, Wilson GV, Provart NJ. 2007. An “Electronic Fluorescent Pictograph” browser for exploring and analyzing large-scale biological data sets. *PLoS ONE* 2: e718.
- Wolf S. 2017. Plant cell wall signalling and receptor-like kinases. *Biochemical Journal* 474: 471–492.
- Xiao Y, Stegmann M, Han Z, DeFalco TA, Parys K, Xu L, Belkhadir Y, Zipfel C, Chai J. 2019. Mechanisms of RALF peptide perception by a heterotypic receptor complex. *Nature* 572: 270–274.
- Yamaguchi Y, Huffaker A, Bryan AC, Tax FE, Ryan CA. 2010. PEPR2 is a second receptor for the Pep1 and Pep2 peptides and contributes to defense responses in Arabidopsis. *Plant Cell* 22: 508–522.
- Zhang LS, Kars I, Essenstam B, Liebrand TWH, Wagemakers L, Elberse J, Tagkalaki P, Tjoitang D, van den Ackerveken G, van Kan JAL. 2014. Fungal Endopolygalacturonases are recognized as microbe-associated molecular patterns by the Arabidopsis Receptor-Like Protein RESPONSIVENESS TO BOTRYTIS POLYGALACTURONASES1. *Plant Physiology* 164: 352–364.
- Zhang W, Fraiture M, Kolb D, Loeffelhardt B, Desaki Y, Boutrot FFG, Toer M, Zipfel C, Gust AA, Brunner F. 2013. Arabidopsis RECEPTOR-LIKE PROTEIN30 and receptor-like kinase SUPPRESSOR OF BIR1-1/EVERSHED mediate innate immunity to necrotrophic fungi. *Plant Cell* 25: 4227–4241.
- Zhou F, Emonet A, Déneraud Tendon V, Marhavy P, Wu D, Lahaye T, Geldner N. 2020. Co-occurrence of damage and microbial patterns controls localized immune responses in roots. *Cell* 180: 440–453.e418.

Supporting Information

Additional Supporting Information may be found online in the Supporting Information section at the end of the article.

Fig. S1 *Fusarium* elicitor responses in additional plant species.

Fig. S2 Characterization of *Fusarium* elicitor responses.

Fig. S3 Root versus shoot responses to fungal elicitors.

Fig. S4 *Fusarium* crude elicitor responses in WT and *fer1* mutants.

Fig. S5 Visualization of recombinant MIK2-cMyc protein in *fer1/MIK2-cMyc*.

Fig. S6 *Fusarium oxysporum* infection assays.

Fig. S7 ROS response measurements in basal immunity-relevant mutant genotypes and MIK2-complemented plants to an enriched *T. atroviride* elicitor fraction.

Fig. S8 Elicitor responses of CWI-sensing and related mutants.

Fig. S9 Visualization of recombinant MIK2-cMyc protein variants from *N. benthamiana* protein extracts.

Fig. S10 EnFOE-induced BAK1-MIK2 association.

Table S1 Plant lines used in this study.

Table S2 Primers used in this study.

Please note: Wiley Blackwell are not responsible for the content or functionality of any Supporting Information supplied by the authors. Any queries (other than missing material) should be directed to the *New Phytologist* Central Office.



About New Phytologist

- *New Phytologist* is an electronic (online-only) journal owned by the New Phytologist Foundation, a **not-for-profit organization** dedicated to the promotion of plant science, facilitating projects from symposia to free access for our Tansley reviews and Tansley insights.
- Regular papers, Letters, Viewpoints, Research reviews, Rapid reports and both Modelling/Theory and Methods papers are encouraged. We are committed to rapid processing, from online submission through to publication 'as ready' via *Early View* – our average time to decision is <26 days. There are **no page or colour charges** and a PDF version will be provided for each article.
- The journal is available online at Wiley Online Library. Visit **www.newphytologist.com** to search the articles and register for table of contents email alerts.
- If you have any questions, do get in touch with Central Office (np-centraloffice@lancaster.ac.uk) or, if it is more convenient, our USA Office (np-usaoffice@lancaster.ac.uk)
- For submission instructions, subscription and all the latest information visit **www.newphytologist.com**